Energy

http://www.aimspress.com/journal/energy

Research article

Analysis of a hydrostatic drive wind turbine for improved annual energy production

Majid Deldar[1], Afshin Izadian[2] and Sohel Anwar[3],*

[1] Meggitt Control Systems, Los Angeles, CA 91605, USA
[2] Energy Systems and Power Electronics Lab, Purdue School of Engineering and Technology, Indianapolis, Indiana, USA
[3] Department of Mechanical and Energy Engineering, Purdue School of Engineering and Technology Indianapolis, Indiana, USA

* Correspondence: Email: soanwar@iupui.edu; Tel: +13172747640.

Abstract: This paper presents an analysis on ways to improve the annual energy production (AEP) of a wind turbine utilizing a drivetrain that operates based on the hydrostatic transmission. The system configuration of such a drivetrain is explained in details and a comparison of operation and characteristics with existing drivetrains is provided. AEP was estimated for these configurations through appropriate dynamic modeling and operational efficiency optimization. Optimal selection of a number of design variables and system parameters contributed to the improvements in the AEP. Findings of this study demonstrate that the proposed hydrostatic drivetrain improves the AEP of a 750 kW turbine by up to +8% when compared with a geared wind turbine. The AEP improvements of the hydrostatic drive wind turbine were more than 10% for a 1.5 MW system over geared configuration. It is also demonstrated that the efficiency of power generation can be improved under various wind speeds. The suitable selection of synchronous speed of the generator directly improves the efficiency of operation by up to 35% at low wind speeds. An efficiency improvement was also observed under higher operating pressures and longer turbine blades.

1. Introduction

By 2030, the wind energy is planned to cover significant share of the US energy [1]. Improving the performance of wind turbine operation results in a higher energy production over time. Conventional gearbox system transmits the power from a high torque-low speed rotor shaft to a low torque-high speed generator shaft. This subassembly is heavy and expensive [2] causing long failure downtime [3]. The variable speed on the generator shaft raises the need for a power electronic converter to adjust the frequency variations. However, hydrostatic transmission system (HTS) can be an alternative power transmission with inherent advantages. The system introduced in this paper is comprised of a fixed displacement pump coupled with the rotor within the nacelle and a variable displacement motor coupled with a generator on the ground level.

In this configuration controlling the displacement of motor adjusts the transmission ratio which consequently sets the generator speed to a synchronous speed. Therefore, the power electronic converters can be eliminated from the drivetrain. To maintain the frequency, the displacement of the hydraulic motor is controlled. The speed of hydraulic pump which varies by the variable speed of wind can be controlled to track the maximum power point. The efficiency of HTS utilized in wind turbines (HTSWT) specifically at low wind speed operations has been studied by Thul et al. [4] and Schmitz el at. [5]. To maximize the transmission system efficiency, Schmitz suggests a switching mechanism between two hardware configurations, one with smaller pumps and motors (set to have high efficiency at low wind speeds) and one with larger pumps and motors (set to have high efficiency at high wind speeds). However, the transition between the sets of low and high speed imposes large breaking torque on hydrostatic components. Dutta [6] suggested an auxiliary pump to be used to store pressurized flow in an accumulator. This stored energy can be released when wind speed is slightly lower than rated speed. Although this approach can increase AEP, the issue of low efficiency at low wind speeds has not been addressed. The effect of system parameters such as the synchronous speed of the generator and the blade size as well as its operating conditions on the efficiency of hydrostatic wind turbines have not been studied before.

In this paper, efficiency improvement techniques in a wind turbine drivetrain with hydrostatic transmission system are investigated. The design of the turbine is optimized to achieve higher efficiency resulting in an increased annual energy production (AEP). The AEP of the optimized wind turbine is simulated and compared with conventional wind turbines with gearbox to demonstrate the benefits.

The paper is organized as follows: In section II, the hydrostatic transmission system is utilized for the wind turbine drivetrain and the governing equations are shown. In section III, the effect of regional operating conditions on the efficiency improvements is discussed. In section IV, the effect of synchronous speed on the efficiency improvements are discussed. In section V, the effect of operating pressure and rotor blade on the efficiency is discussed. The power generation and annual energy production are discussed in sections VI and VII. A comparison is provided with the existing drivetrains in section VII.

2. Hydrostatic transmission system for wind turbine applications

Hydraulic pumps and motors are the key components of a hydrostatic circuit of power transmission. Figure 1 shows the proposed configuration of the hydrostatic drivetrain wind turbine where the turbine shaft drives a hydraulic pump providing high pressure flow to the circuit. On the motor side, the generator torque that imposes load on the hydraulic motor shaft induces pressure

between the pump outlet and the motor inlet, i.e. the high pressure line shown in Figure 1. The motor rotates the generator shaft and a low pressure line completes the hydrostatic circuit. Pumps and motors have similar structure as both convert mechanical energy to hydrostatic energy and vice versa. To investigate the system operating principles and study the efficiency, the torque balance in a hydraulic machine can be written as follows [9–11]:

$$T_L = D_m P - C_{vm} D_m \omega_m - C_{fm} D_m P - T_{Cm} \tag{1}$$

$$Q_m = D_m \omega_m + K_{Sm} P \tag{2}$$

where P is the pressure, T_L is the generator load torque, D_m and ω_m are the motor displacement and speed respectively. C_{vm} and C_{fm} are viscous drag and coulomb friction coefficient respectively, and T_{Cm} is the breakaway torque. The term $D_m P$ in Eq 1 is the driving torque of the motor and the other three terms show mechanical losses. In addition, a portion of fluid slips from high pressure chamber to the low pressure chamber of the pump or motor. Therefore, the actual required flow rate slightly differs from the theoretical value. This volumetric loss within a motor is explained in Eq 2. In this equation, Q_m is the actual flow of motor and K_{Sm} is the slippage coefficient of motor. Similarly for the pump, mechanical loss and volumetric loss [9–11] are written as follows:

$$T_R = D_P P + C_{Vp} D_P \omega_{rotor} + C_{Fp} D_p P + T_{Cp} \tag{3}$$

$$Q_p = D_P \omega_p - K_{Sp} P \tag{4}$$

where, T_R is the torque of the turbine rotor, D_p and ω_P are pump displacement and speed respectively, C_{vp} and C_{fm} are viscous drag and coulomb friction coefficient respectively and T_{Cp} is the breakaway torque. In Eq 4, Q_p is the actual flow of the pump and K_{Sp} is the slippage coefficient.
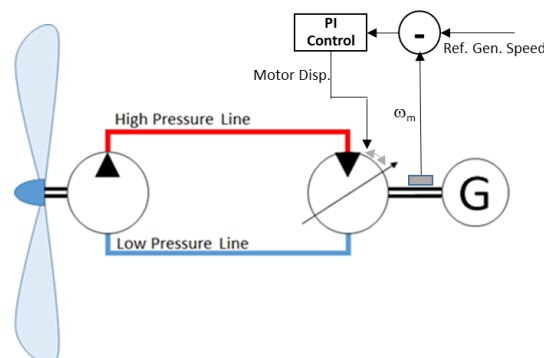
Figure 1. Schematic of a wind turbine utilizing HTS. This drivetrain does not have a power electronic converter as the speed of the generator is closely controlled by the displacement. The control system and the interface of the electrical and mechanical systems are shown.

3. Effect of regional operating conditions on overall efficiency

From motor and pump models 1–4, it can be seen that the energy conversion efficiency is influenced by the mechanical and volumetric losses. The mechanical losses are viscous drag, coulomb friction and breakaway torque. Viscous drag is caused by the fluid shear between two parts having relative motion. The coulomb friction is due to contact between two metal surfaces such as bearing and shaft and the breakaway torque is caused by sealing friction. Overall efficiency of a pump and a motor including losses [9–11] are formulated as follows:

$$\eta_p = \frac{1 - \dfrac{K_{Sp}}{A}}{1 + A C_{vp} + C_{fp} + \dfrac{T_{cp}}{D_p P}}, \quad A = \frac{\mu \omega_p}{P} \tag{5}$$

$$\eta_m = \frac{1 - B C_{vm} - C_{fm} - \dfrac{T_{cm}}{D_m p}}{1 + \dfrac{K_{Sm}}{B}}, \quad B = \frac{\mu \omega_m}{P} \tag{6}$$

where η_p and η_m are the overall efficiencies of pump and motor respectively and μ is the dynamic viscosity of the fluid. Figure 2 illustrates a generic trend of pump and motor efficiency as a function of factor A or B. This factor is a function of the ratio of speed over pressure. The efficiency trends for a hydraulic motor and a hydraulic pump typically follow similar trends.
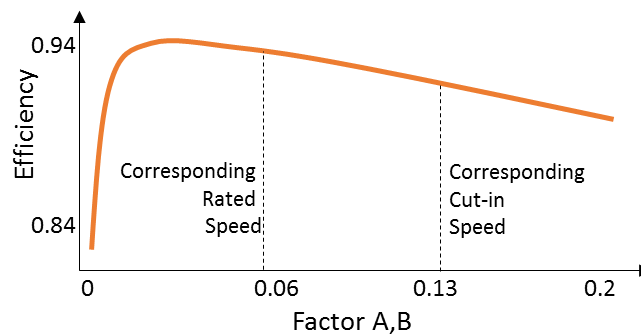
Figure 2. General trend of efficiency variation for a pump (A) or a motor (B) [8].

The efficiency is affected by rotational speed and pressure variations. In applications where operating conditions, pressure and speed do not vary widely, the hydrostatic transmission is designed to have the best efficiency. However, due to intermittent nature of wind, the operating conditions change widely and it becomes impossible to continuously operate the system at its maximum efficiency. Therefore, the system operation can be designed to reach maximum efficiency at higher input powers and maintain efficiency as much as possible when power input drops. Accordingly, the wind power and turbine characteristics are obtained as follows. The amount of power that a wind turbine can extract from wind is determined [12,13] by:

$$p = \left(\frac{1}{2}\pi\rho\right)C_p R^2 V^3 , \tag{7}$$

where p is the rotor power, ρ is the air density, C_p is the power coefficient of turbine, R is the radius of rotor, V is the instantaneous wind speed, and $\lambda = \dfrac{R\ \omega_p}{V}$ is the instantaneous tip-speed-ratio of the rotor.

Considering $T_R = \dfrac{p}{\omega_p}$, the rotor torque can be expressed as follows:

$$T_R = \left(\frac{1}{2}\pi\rho\right)C_p\left(\frac{R^5}{\lambda^3}\right)\omega_p^2 \tag{8}$$

The rotor driving torque equals the braking torque applied on the pump shaft as $T_p = T_R$, where $T_p = \dfrac{D_p\ P}{\eta_{Pmech}}$, with $\eta_{Pmech.}$ being the mechanical efficiency of the pump. Hence, the operating pressure of the transmission fluid becomes proportional to the square of rotor shaft speed as follows:

$$P = \left(\eta_{Pmech}\frac{1}{2}\pi\rho C_p\frac{R^5}{\lambda_{opt}}\right)\frac{\omega_p^2}{D_p} \tag{9}$$

Tracking maximum power point requires maintaining the tip-speed-ratio at an optimum value, λ_{opt}, where C_p is maximum (as illustrated in Figure 3). While a linear correlation of the turbine shaft speed with the wind speed can be obtained by maintaining $\lambda = \lambda_{opt}$, the operating pressure P is a quadratic function of turbine shaft speed, according Eq 9.
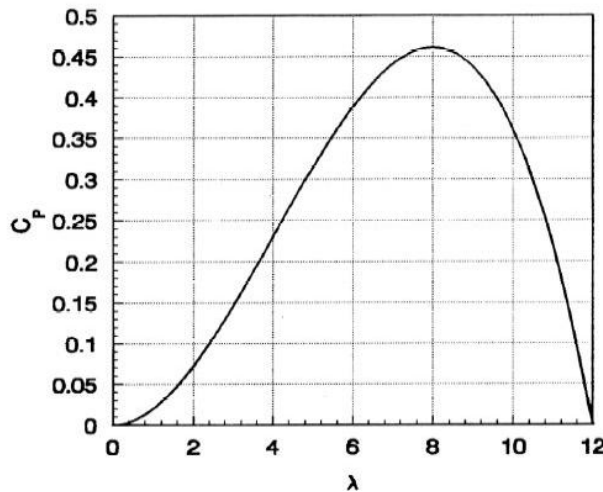
Figure 3. A representative Cp—λ curve for a wind turbine [25].

Considering dimensionless factor A, at higher wind speeds, the denominator (operating pressure) increases faster than the increase of the numerator. Therefore, factor A becomes smaller at higher wind

speeds. This creates an optimum operation region as illustrated in Figure 2. In this optimum region, the operating efficiency uniformly increases as the wind speed increases from the cut-in to the rated wind speed where at it reaches the maximum efficiency within the range.

In factor *B*, which determines motor efficiency, the numerator is constant since motor speed is desired to be maintained regardless of the wind speed. Pressure varies quadratic with wind speed, hence, the value of factor *B* decreases faster at higher wind speed. This suggests that motors follow a similar operational planning to the pump.

In this section, it was explained that the efficiency of hydrostatic transmission depends on the operating conditions. To achieve higher efficiencies at low wind speeds, the characteristics of the turbine (prime-mover) and the generator (load) must be considered in conjunction with HTS operation characteristics. Therefore, in the next sections, the efficiency is measured against the generator speed and the operating pressure variations.

4. Effect of generator's synchronous speed on the overall efficiency

To increase the overall energy conversion efficiency, both mechanical efficiency $\eta_{mech.}$, and the volumetric efficiency η_{vol} should be improved. Hydrostatic parameters that affect the efficiency are: Pressure, pump/motor speeds, and displacements. Pump displacement is a constant value but its speed is controlled to maintain the optimum tip-speed-ratio. Thus, this parameter cannot be controlled for efficiency improvement. Effects of motor displacement and pressure are analyzed here to suggest approaches for efficiency improvements.

The motor efficiency as a function of motor displacement is strictly increasing as observed in Eq 6. This means that larger motor displacement improves motor efficiency. The optimality of this relationship between efficiency variations and motor displacement is derived using the following partial derivative:

$$\frac{\partial \eta_m}{\partial D_m} = \frac{\dfrac{T_{cm}P}{(D_m P)^2}}{\left(1+\dfrac{K_{Sm}}{B}\right)^2} > 0 \tag{10a}$$

Also, the hydrostatic drivetrain efficiency is obtained as:

$$\eta_{HST} = \eta_p * \eta_m \tag{10b}$$

The hydraulic flow rate is determined by pump speed. To maintain higher efficiency, the same amount of flow, when received by the motor at a large displacement, exhibits a reduced shaft speed. This imposes a larger number of pole pairs in the generator to maintain the 60 Hz frequency. Considering high speed generators as reported in [7], when a 1500 rpm 50 Hz generator [5] or an 1800 rpm 60 Hz generator was used, low efficiencies were reported at low wind speeds.

The efficiency of the hydrostatic drivetrain of the wind turbine is simulated at various wind speeds using Eq 1–Eq 10. Figure 4 illustrates the effect of reducing the synchronous speed of generators (ω_m) on the wind turbine drivetrain efficiency. This figure shows that the efficiency of system from the turbine shaft to the generator shaft can be increased when a lower synchronous speed generator is selected. This is more evident at low wind speed operations, such that the efficiency can be improved from a 46% for 1800 rpm generator to 74% in case of a 600 rpm generator. In these simulations, the turbine and pump specifications remained constant and the generator speed was regulated in all wind speeds. Specifications of the rotor and pump that was used for the simulations are summarized in Table 1.
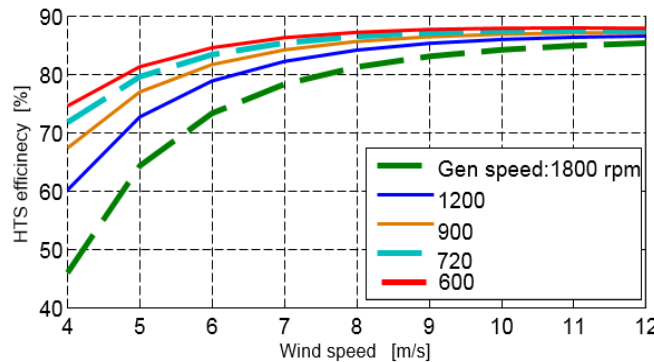
Figure 4. Effect of generator speed on HTS efficiency.

Table 1. Turbine and pump specifications.

Turbine	Rated power (kW)	600
	Diameter (m)	48
	Maximum power coefficient	0.475
	Optimum TSR	7
	Cut-in speed (m/s)	4
	Rated wind speed (m/s)	12
Pump	Displacement (lit/rev)	43.600
	Max pressure (bar.)	300
	Speed range (rpm)	10–30

5. Effect of operating pressure and blade radius on the overall efficiency

Another approach to increase the efficiency of HTS is to increase the operating pressure specifically at low wind speeds. Increasing the driving torque reduces the percentage of torque loss over the driving torque, which causes mechanical efficiency improves. However, the overall efficiency improvement is not always obtained as higher pressures reduce the volumetric efficiency. Considering a constant speed for generator, higher pressures reduce the factor *A* in Eq 5. When the pressure reaches a certain value, reduction in volumetric efficiency exceeds the improvement in mechanical efficiency. As a result, the overall efficiency deviates from its maximum point. To ensure that the increasing

pressure improves the efficiency, a HTS is designated to operate in optimum regions shown in Figure 2. The point of maximum efficiency is obtained analytically for the motor as follows (similar argument is applied to the pump):

$$\frac{\partial \eta_m}{\partial P} = \frac{\dfrac{D_m \mu \omega_m C_{vm} + T_{cm}}{D_m P^2} + \dfrac{2 C_{vm} K_{sm}}{P} + \dfrac{K_{sm}\left(2 T_{cm} + C_{fm} - K_{sm}\right)}{D_m \mu \omega_m P}}{\left(1 + \dfrac{K_{Sm}}{B}\right)^2} \tag{11}$$

Sign of $\frac{\partial \eta_m}{\partial P}$ is determined by summation of the three terms in the numerator. The term $\frac{D_m \mu \omega_m C_{vm} + T_{cm}}{D_m P^2}$ is always positive but its value is decreased at very high pressure since its denominator increases quadratic with pressure. The term $\frac{2 C_{vm} K_{sm}}{P}$ is also positive. However, the sign of the third term, $\frac{K_{sm}\left(2 T_{cm} + C_{fm} - K_{sm}\right)}{D_m \mu \omega_m P}$, can be either positive or negative. If the third term is positive, all of terms of the partial derivate are positive and hence the overall efficiency of motor is a strictly increasing function of pressure. However, Breakaway torque, T_{cm} and coulomb friction, C_{vm} are usually smaller than the slippage coefficient, K_{sm}. Thus, the third term of the partial derivate can become negative. The following argument illustrates that from low to a medium pressure, the overall efficiency is strictly increasing with pressure.

At low to medium pressures:

$$\begin{cases} \dfrac{D_m \mu \omega_m C_{vm} + T_{cm}}{D_m P^2} > 0 \\[2mm] \dfrac{2 C_{vm} K_{sm}}{P} > 0 \\[2mm] \dfrac{K_{sm}\left(2 T_{cm} + C_{fm} - K_{sm}\right)}{D_m \mu \omega_m P} < 0 \end{cases} \Rightarrow \frac{\partial \eta_M}{\partial P} > 0 \tag{12}$$

At high pressure:

$$\begin{cases} \dfrac{D_m \mu \omega_m C_{vm} + T_{cm}}{D_m P^2} \approx 0 \\[2mm] \dfrac{2 C_{vm} K_{sm}}{P} > 0 \\[2mm] \dfrac{K_{sm}\left(2 T_{cm} + C_{fm} - K_{sm}\right)}{D_m \mu \omega_m P} < 0 \end{cases} \Rightarrow \frac{\partial \eta_M}{\partial P} < 0 \tag{13}$$

Hence, at high pressure, the drivetrain efficiency decreases as the pressure increases. From low to medium pressure, the effect of mechanical efficiency overcomes the effect of volumetric efficiency. However, at high pressure, the effect of volumetric efficiency dominates. The HTS should be designed to operate in the region where efficiency increases by pressure.

To increase the pressure at low wind speeds, a large driving torque (prime-mover) is required. Based on wind turbine power-torque characteristics, a larger swept area generates higher torque, as indicated by Eq 7. Assuming that the wind turbine is designed for a fixed power rating, a larger swept

area helps the turbine reach the rated power at a lower wind speed. Figure 5 illustrates the correlation between the blade radius, R, the rated wind speed and turbine rated power.
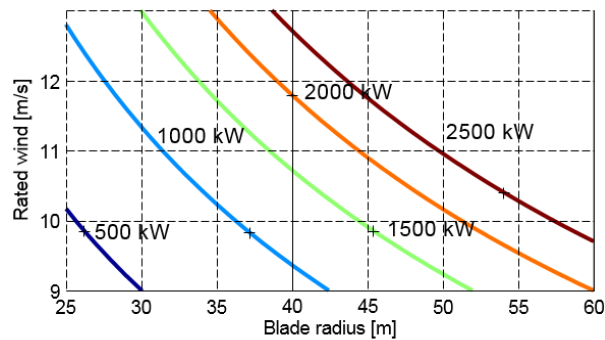

Figure 5. Power rating at different blade radius and rated wind speed.

As Figure 5 demonstrates, different combination of blade radius and rated wind speed might yield a specific power rating. For instance, 1000 kW power can be generated with blade radius of 30 m in a geographic area with rated wind speed of 11.4 m/s. It was observed in Eq 8 that the rotor torque was proportional to R^5. Hence, the torque generation enhancement at low wind speeds can be achieved by using larger blades. Figures 6 and 7 demonstrate the power and torque curves of a wind turbine rated at 600 kW when utilizing different blade radius and wind rated speeds.
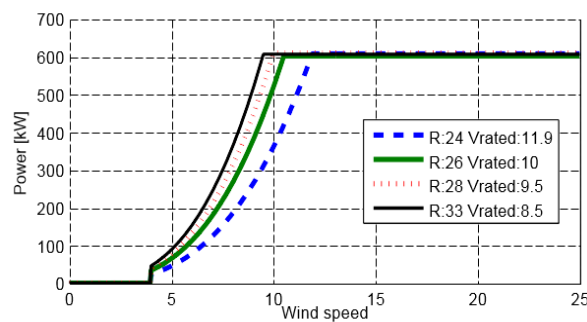

Figure 6. Power curve of a 600 kW turbine considering various blade radius.
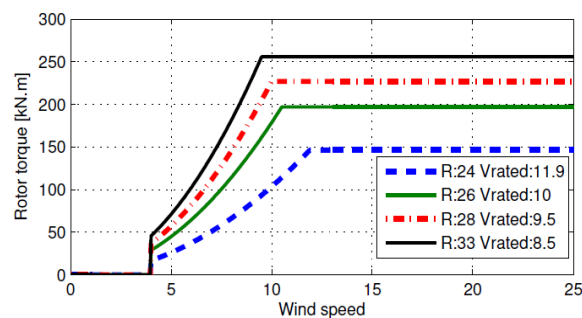
Figure 7. Torque curve of a 600 kW turbine considering various blade radius.

As illustrated in Figures 6 and 7, at a specific turbine power rating, a configuration with larger blade generates higher torque at lower wind speed. This enables the pump and motor to operate at a higher pressure and consequently improve the efficiency. The drivetrain efficiency is again simulated against wind speed in Figure 8 where the overall efficiency of the hydrostatic drivetrain is compared under various blade length. At low wind speeds the efficiency was improved by 5% when the blade size was increased. This produced more torque at low rpm.

It can be concluded that a configuration of wind turbine with longer blades yields higher efficiency especially at lower wind speeds.
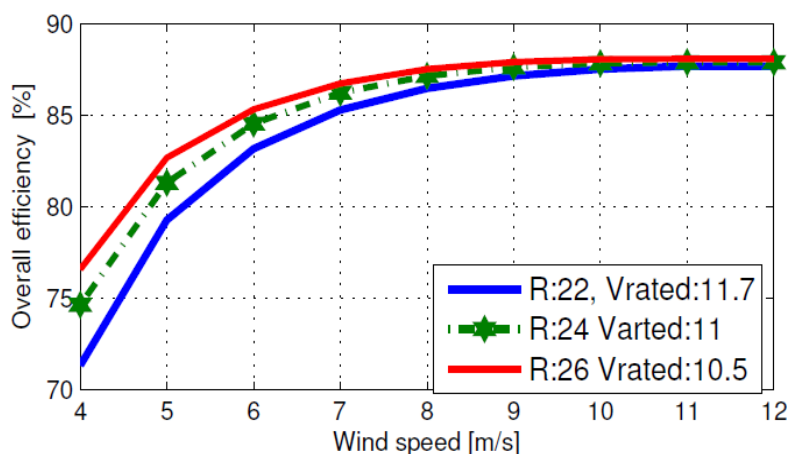
Figure 8. Overall efficiency of a 600 kW with different combination of rated wind speed and blade radius.

6. Enhancing capacity factor using larger swept area (longer blades)

In previous sections, different techniques were introduced to improve the efficiency of pumps and motors. Considering these technological advantages, a side-by-side comparison of the proposed hydrostatic drivetrain with existing drivetrains over the power generation and annual energy production is necessary. The output powers from the proposed hydrostatic drivetrain wind turbine is now compared against the power curves obtained from the wind turbine by Carrillo et al. in [13]. The wind turbines of both systems have the same rotor rated at 1500 (kW) and the blade radius of 38.5 (m). The power generation as a function of wind speed is shown in Figure 9. The difference between the power generations between HTSWT and geared WT is show in Figure 10. This demonstrates that at wind speeds close to cut-in and rated, the proposed hydrostatic transmission system has a better power profile.
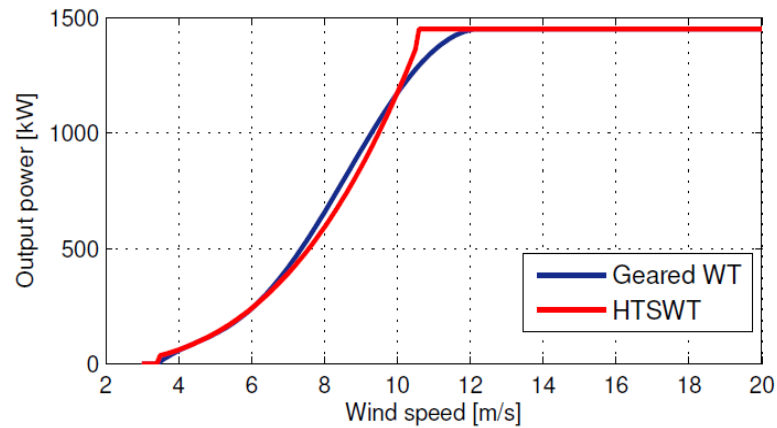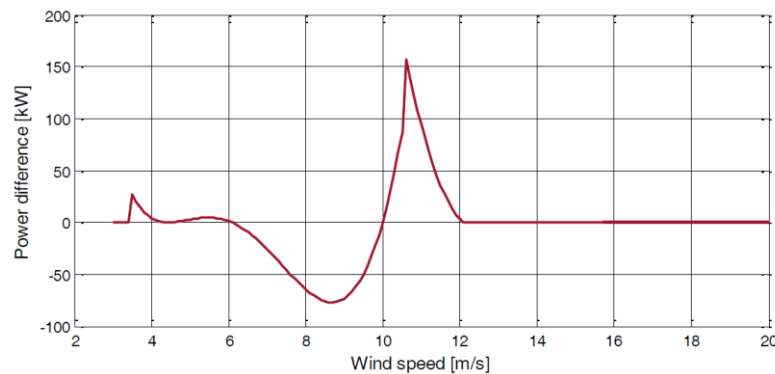
Rated power: 1500 kW, R_{blade}: 38.5, $C_{p\,max}$: 0.4825

Closer to cut-in speed, C_p deviation impacts P_{out} of a geared WT

In moderate winds, higher transmission efficiency is in favor of geared WT

Closer to rated wind, again C_p deviates from the maximum for a geared WT

**Figure 9.** Output power comparison between a geared WT and a HTSWT (in kW).

Figure 10. Relative power comparison of a HTSWT and a geared WT (power rating 1500 kW with R_{blade} 38.5).

The following observations are made:

(1) In wind speed range near cut-in and rated, the rotor of the conventional system cannot track maximum power due to restriction on minimum and maximum speeds imposed by doubly fed induction generators (DFIG), also reported in [14].

(2) In the proposed wind turbine and drivetrain the shafts of rotor and generator are decoupled. This allows rotor to track maximum wind power at any wind speed and for the generator to be regulated at a fixed speed.

(3) At median wind speeds, 6–10 (m/s), higher efficiency of gearbox results in higher overall efficiency.

(4) As shown in previous section, using larger swept area improves the HTS efficiency specifically at low wind speed. Here it is discussed that larger swept area also enhance the capacity factor. To elaborate the reasoning for such a claim, wind speed probability distribution is explained. Then effects of rated wind speed and annual mean wind speed on capacity factor or AEP are identified.

Long term wind speed profile is assumed to follow Weibull distribution and, depending on mean wind speed, its scale factor varies while the shape factor is usually around 2 [18]. Regarding probability density function (PDF) of Weibull distribution, at constant shape factor, scale factor determines probability magnitude of the most frequent wind and probability of wind speeds near this wind speed. Figure 11 shows PDF for different scale factors while the shape factor equals two for all of them. As seen in the this figure, greater scale factors tend to reduce the probability magnitude of the most frequent wind speed and shift it to greater wind speeds. Also, greater scale factor is indicator of more evenly distribution around the probability peak.
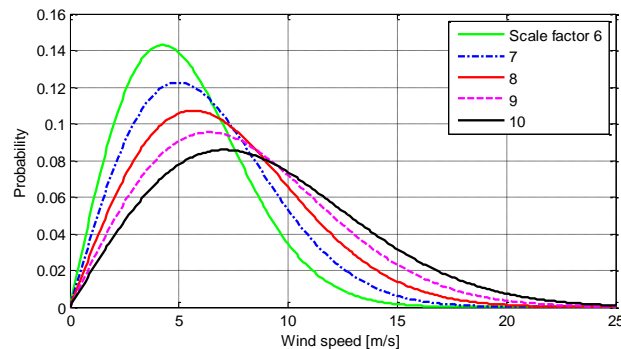
Figure 11. Weibull distribution PDF for different scale factors (shape factor = 2 for all PDFs).

Annual mean wind speed is close to the scale factor thus in wind farms sites where the annual mean speed is greater, higher wind speeds are experienced. In areas where experience greater annual wind speed, setting the rated wind speed at high wind speed can yield higher energy production annually. However, higher rated wind speed can reduce the capacity factor. This phenomenon can be realized by looking at cumulative density function (CDF) of Weibull distribution with different scale factors. The probability associated to each wind speed resulted from various annual mean wind speed is shown in Figure 12.
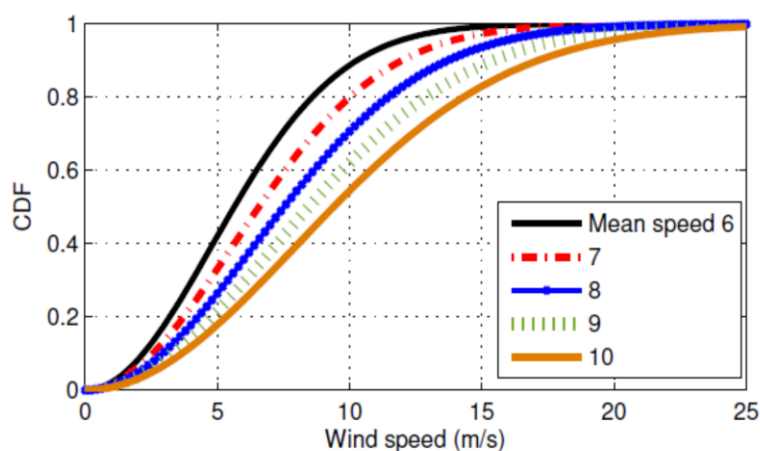

Figure 12. Wind speed probability (CDF) at different mean wind speed for different scale factors (shape factor 2 applied for all).

As seen in Figure 12, for smaller scales factors, the accumulative probability reaches the unit value at lower wind speed. Hence, if the rated wind speed is set at lower wind speed, probability of occurrence for wind speed higher than the rated speed is greater. This is in favor of capacity factor. Analytically, this phenomenon can be explained by looking at definition of capacity factor and Weibull distribution. Capacity factor can simply be defined as:

$$Capcity\,factor = \frac{\displaystyle\sum_{V_i=cut-in}^{cut-out} \left(f_{V_i} \, P_{wr}\big|_{V_i} \right)}{P_{wr}\big|_{Vrated}} \tag{14}$$

where, f_{V_i} is the probability of occurrence for wind speed V_i, P_{wr} is the output power at V_i and V_{rated} is the rated wind speed. Setting V_{rated} at smaller values, reduces the denominator. Also, as explained in Section V and demonstrated in Figure 6, for specific power rating, lower V_{rated} increases output powers at wind speeds closer to the cut-in speed. Consequently, capacity factor is higher for smaller rated wind speed.

Figure 13 shows that capacity factor is improved when the rated wind speed is set at lower values. This observation applies to wind turbines with any types of transmission. For wind turbines with HTS, as discussed in Section V, this is also in favor of HTS efficiency improvement.
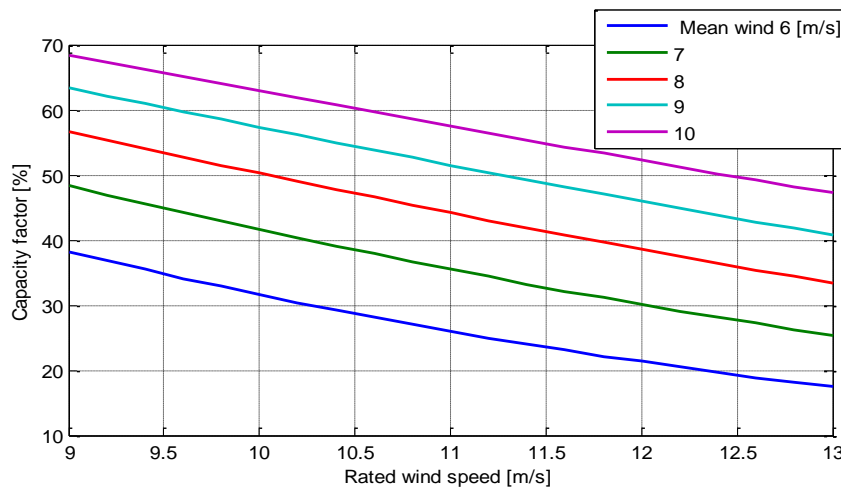
Figure 13. General trend of capacity factor variation with respect to rated wind speed at different annual mean wind speeds.

In Section V, it was analytically proved that optimizing operation planning can improve the efficiency of HTS. In this section, effect of rotor power characteristics on the capacity factor was elaborated. In the next section, the overall annual energy production (AEP) of a wind turbine with HTS will be compared with geared wind turbines. These system can be compared accurately when identical conditions apply on them. As a result, the AEP will give a distinctive metric to compare these systems.

7. Annual energy production and comparison with existing technologies

7.1. Annual energy production

Figure 10 demonstrated a dependency of power generation differences to wind speeds. However, annual energy production (AEP) considers a spectrum of wind speeds and becomes a reliable measure of the system performance [2,11,15,24]. AEP estimates the accumulated energy production from a wind turbine considering the power curve of the given wind turbines and the probability of all wind speeds in one year [16,17].

Considering similar turbine specifications, the AEPs were compared at different annual mean wind speeds. At each annual mean wind speed, the same scale factor and shape factor applied to both plants (the hydraulic drivetrain and a gearbox system). The wind speed turbulence is not considered in AEP calculation. The turbine's swept area on AEP was investigated. The comparisons were performed at generators in two power ratings of 750–900 kW and 1500–1700 kW. The rotor specifications and the power curves of conventional turbine that used for the comparison are listed in Table 2 [13,19] and Table 3.

Table 2. Specifications of three turbines used for AEP comparison 750–900 Kw wind turbines.

Rated Power (kW)	Rotor rad. (m)	Max C_p	Cut-in Speed (m/s)	Rated Speed (m/s)
750	26	0.468	4	11.7
850	29	0.487	4	11
900	32	0.482	4	11

**Table 3.** Specifications of three turbines used for AEP comparison 1500–1700 kw wind turbines.

Rated Power (kW)	Rotor rad. (m)	Max C_p	Cut-in Speed (m/s)	Rated Speed (m/s)
1500	35	0.461	3.5	12.7
1600	38.5	0.459	3.5	12
1700	41.2	0.482	3.5	11.4

The % AEP difference (HSTWT AEP-Geared WT AEP) was simulated at various annual mean wind speeds. The results are shown in Figure 14 which demonstrates that the proposed wind turbine and transmission system with a 32 m rotor radius generates 3–7% higher energy in average than a conventional system. Similarly, a system with 29 m blade yields up to 6% higher energy than a conventional wind turbine. In case of a 26 m radius turbine, operating over a lower range of annual mean wind speeds (up to 7.7 m/s), the proposed system generated less energy than a conventional system while at higher wind speeds the proposed system produced higher energy. In addition, comparing the trend of AEP variations with respect to the radius, it is observed that larger rotor radius contributed to comparatively higher energy production of the proposed system.
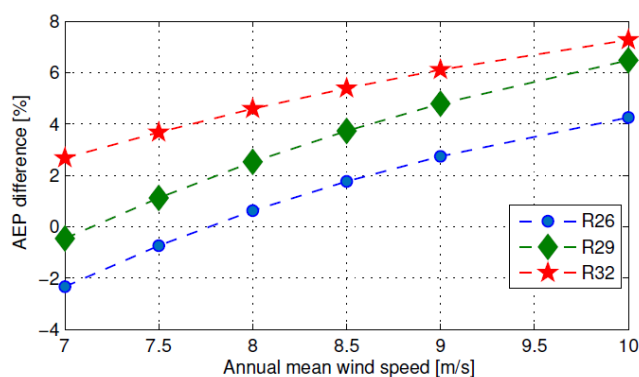
Figure 14. AEP improvement of a HTS compared with a conventional WT, power rating: 750–900 kW.

Similar simulation comparisons were performed on a wind turbine of higher power rating (1500–1700 kW). AEP of three size rotors (listed in Table 3) were compared and the results are shown in Figure 15. This graph also demonstrates that the AEP yield is higher for the proposed hydrostatic drivetrain wind turbines than the conventional ones. Additionally, improvement on AEP yield is greater for larger radii wind turbines as observed in this plot.
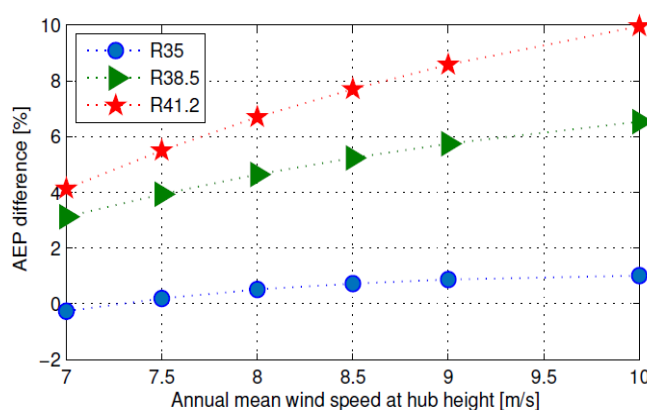
Figure 15. AEP improvement of a HTSWT compared with a conventional WT, power rating: 1500–1700 kW.

7.2. Comparison with existing technologies

A comparison of the % AEP difference (HSTWT AEP-Geared or direct drive WT AEP) was simulated at various annual mean wind speeds for two existing geared WT systems. The results shown in Figure 16 which also demonstrated that the proposed system collects more energy annually than the existing wind turbine drivetrains. Figure 16 shows the proposed hydrostatic wind turbine compared with the GE (with gearbox) and Vensys (direct-drive). As the figure demonstrates, a significantly higher annual energy production (~8%) is expected from the proposed wind turbine, when it is installed in geographical locations with mean wind speeds higher than $6\frac{m}{s}$. Compared to the systems with a gearbox, it demonstrated a superior AEP capability, comparable with the direct-drive.
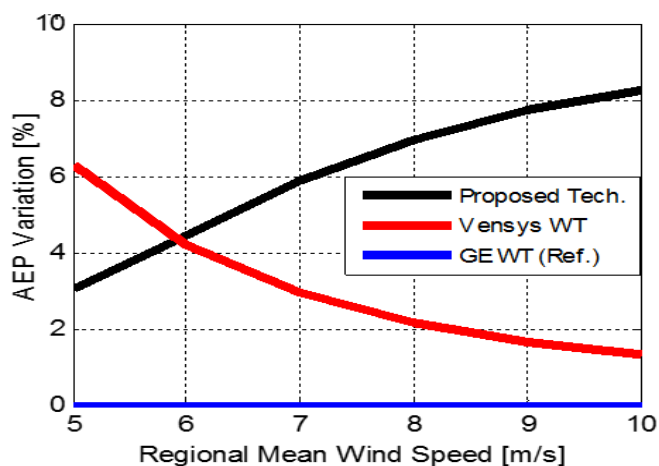
Figure 16. AEP comparison of the proposed technology with the wind turbine driven by gearbox and a direct drive system.

8. Conclusions

This work demonstrated that optimal selection of a number of design variables and system parameters is critical to enhancing the efficiency of a hydrostatic drive wind turbine. To achieve such efficiency improvement that would result in higher AEP, the synchronous speed of generators must be selected properly, the length of blades must be adjusted optimally, and the system operation must be optimized. The efficiency enhancement particularly at low wind speeds resulted in higher annual energy production for the proposed drivetrain. It was shown that the proposed system could generate more power than a gearbox driven drivetrain and a direct drive wind turbine, by up to 8–10%. Specifically, the simulation results demonstrated that the proposed hydrostatic drivetrain improves the AEP of a 750 kW turbine by up to +8% when compared with a geared wind turbine. The AEP improvements of the hydrostatic drive wind turbine were more than 10% for a 1.5 MW system over geared configuration. Additionally, appropriate selection of synchronous speed of the generator directly improves the efficiency of HSTWT operation by up to 35% at low wind speeds. An efficiency improvement was also observed under higher operating pressures and longer turbine blades.

Acknowledgment

Conflict of interest

All authors declare no conflict of interest in this paper.

References

1. Izadian A, Girrens N, Khayyer P (2013) Renewable energy policies, A brief review of the latest U.S. and E.U. policies. *IEEE Ind Electron Mag* 7: 21–34.

2. Tegen S, Hand M, Maples B, et al. (2012) 2010 cost of wind energy review. *No. NREL/TP-5000-52920*. National Renewable Energy Lab. (NREL), Golden, CO, United States.

3. Sheng S (2013) Report on wind turbine subsystem reliability-a survey of various databases. NREL/PR-5000-59111. Golden, CO: National Renewable Energy Laboratory, Report.

4. Thul B, Dutta R, Stelson KA (2011) Hydrostatic transmission for mid-size wind turbines, In: Proceedings of 52nd National Conference on Fluid Power, Las Vegas, NV, Conference Proceedings.

5. Schmitz J, Vatheuer N, Murrenhoff H (2011) Hydrostatic drive train in wind energy plants. RWTH Aachen University, IFAS Aachen, Germany.

6. Dutta R, Wang F, Bohlmann BF, et al. (2014) Analysis of short-term energy storage for midsize hydrostatic wind turbine. *J Dyn Syst Meas Control* 136: 011007.

7. Merritt HE (1967) Hydraulic control systems. John Wiley & Sons.

8. Fitch EC (2004) Hydraulic component design and selection. Bardyne, Incorporated.

9. Manring N (2005) Hydraulic control systems. John Wiley and Sons Incorporated.

10. Bianchi FD, Battista HD, Mantz RJ (2006) Wind turbine control systems: Principles, modelling and gain scheduling design. Springer.

11. Bhadra SN, Kastha D, Banerjee S (2005) Wind electrical systems. Oxford University Press.

12. Burton T, Jenkins N, Sharpe D, et al. (2011) Wind energy handbook. John Wiley and Sons.

13. Carrillo C, Montano AO, Cidras J, et al. (2013) Review of power curve modelling for wind turbines. *Renew Sust Energ Rev* 21: 572–581.

14. Jonkman J, Butterfield S, Musial W, et al. (2009) Definition of a 5-MW reference wind turbine for offshore system development. CO: National Renewable Energy Laboratory Golden.

15. Manwell JF, Mcgowan JG, Rogers AL (2010) Wind energy explained: Theory, design and application. John Wiley & Sons.

16. Nielsen P, Sorsen T (2006) Windpro software user manual. Alborg, Denmark, EMD International AS, vol. 181.

17. Johnson GL (2006) Wind energy systems. Gary L. Johnson.

18. Mon é C, Stehly T, Maples B, et al. (2015) 2014 cost of wind energy review. In: Lawrence Berkeley National Laboratory Paper LBNL-6A20-64281.

19. West M (2005) Microsoft Excel Wind Analysis Software Program: Instructions and Walkthrough. Available from: https://www.scribd.com/presentation/98726382/Excel-Wind-Analysis-Present.

20. Bryson AE (1975) Applied optimal control: Optimization, estimation and control. CRC Press.

21. Bertsekas DP (2005) Dynamic programming and optimal control. Athena scientific, vol. 1, no. 3. Belmont, MA.

22. Lewis FL, Syrmos VL (1995) Optimal control. John Wiley and Sons.

23. Deldar M (2016) Decentralized multivariable modeling and control of wind turbine with hydrostatic drivetrain. Dissertation, Purdue University.

24. Deldar M, Izadian A, Anwar S (2015) Reconfiguration of a wind turbine with hydrostatic drivetrain to maximize annual energy production. *IEEE Energ Convers Congr Expo* 2015: 6660–6666.

25. Available from: http://mstudioblackboard.tudelft.nl/duwind/Wind%20energy%20online%20 reader/Static_pages/Cp_lamda_curve.htm.